

Demosaicing of Noisy Data: Spatially Adaptive Approach

Dmitriy Paliy^a, Mejdi Trimeche^b, Vladimir Katkovnik^a, Sakari Alenius^b

^aInstitute of Signal Processing, Tampere University of Technology, P.O.Box 553, FIN-33101
Tampere, Finland.

e-mail: firstname.lastname@tut.fi

^bNokia Research Center, Tampere, Finland.

e-mail: firstname.lastname@nokia.com

ABSTRACT

In this paper we propose a novel color demosaicing algorithm for noisy data. It is assumed that the data is given according to the Bayer pattern and corrupted by signal-dependant noise which is common for CCD and CMOS digital image sensors. Demosaicing algorithms are used to reconstruct missed red, green, and blue values to produce an RGB image. This is an interpolation problem usually called color filter array interpolation (CFAI). The conventional approach used in image restoration chains for the noisy raw sensor data exploits denoising and CFAI as two independent steps. The denoising step comes first and the CFAI is usually designed to perform on noiseless data. In this paper we propose to integrate the denoising and CFAI into one procedure. Firstly, we compute initial directional interpolated estimates of noisy color intensities. Afterward, these estimates are decorrelated and denoised by the special directional anisotropic adaptive filters. This approach is found to be efficient in order to attenuate both noise and interpolation errors. The exploited denoising technique is based on the local polynomial approximation (LPA). The adaptivity to data is provided by the multiple hypothesis testing called the intersection of confidence intervals (ICI) rule which is applied for adaptive selection of varying scales (window sizes) of LPA. We show the efficiency of the proposed approach in terms of both numerical and visual evaluation.

Keywords: Bayer pattern, color filter array interpolation, spatially adaptive denoising, sensor noise

1. INTRODUCTION

In digital imaging systems, the image formation is a complex process. The light passes through the optical system of the camera and is focused a digital sensor. The sensor is composed of photon-collection sites covered with a color filter array (CFA). Each site works as a photon-counter to measure the amount of light coming to it. Color filter arrays are used to sample different spectral components, thus each site registers the amount of light at a particular spectral range. The sensor produces a digital value for each site which corresponds to the intensity of the light at that position. This digital output of the sensor is called “raw data”. The Bayer CFA samples the coming light into Red (*R*), Green (*G*), and Blue (*B*) components¹ according to a checkerboard rectangular sampling grid (Fig. 1). It is the most widespread CFA nowadays and, therefore, we focus mainly on it.

It is known that the raw data from the sensor is corrupted by signal-dependant noise². Such modeling is common for charge-coupled device (CCD) and complementary-symmetry/metal-oxide semiconductor (CMOS) digital image sensors. The most widely encountered models are Poisson, film-grain, multiplicative and speckle noise. Their common property is the dependence of the variance of noise from the signal³.

The problem is to restore the true observation scene from the noisy sampled data. The conventional approach used in image restoration chains for raw sensor data exploits successive independent denoising and demosaicing steps. Denoising aims to remove the noise, and demosaicing performs interpolation of missing colors assuming that the processed data is noise free.

In general, the approaches used for Bayer pattern¹ CFAI can be divided in two classes of signal domain methods: the gradient-based methods^{4,5,6,7} and the methods based on filtering of difference between luminance and chrominance channels^{9,10,11,12}.

The algorithms of the first group rely on the idea of edge-directed interpolation. The intraplane correlation is taken into consideration by estimating local gradients. The main assumption is that locally differences between colors ($R-G$) and ($B-G$) are nearly constant. At each pixel the gradient is estimated, and the color interpolation is carried out directionally, based on the estimated gradient.

The directional filtering is the very popular approach for color demosaicing. The directional interpolation scheme by Hamilton and Adams⁶ is perhaps the one of the most popular. The gradients of blue and red channels are used as the correction terms in order to interpolate the green channel. The horizontal and vertical derivatives are calculated and the direction with the smallest derivative is used for interpolation. For interpolation of green channel the mean of the green samples along the selected interpolation direction is used. Once missing green pixels are filled, the red and blue samples are interpolated similarly. Similar idea is exploited in works^{5,7,8} which are different by fusing of vertical and horizontal estimates.

The second group of methods exploits another idea. At the beginning the initial estimates of color channels are obtained. After that the differences between luminance and chrominance channels are exploited in order to remove interpolation errors. Let us give a short overview of some of the most well-known methods in this field.

Gunturk et al.⁹ have proposed thresholding in the wavelet domain of directional high frequency components obtained by the wavelet filter bank decomposition. Hirakawa and Parks in adaptive homogeneity-directed demosaicing algorithm¹⁰ proposed processing in the CIELAB color space by evaluation of so-called homogeneity map. This is done aiming efficient color channel decorrelation. Zhang and Wu¹¹ proposed to find estimates of difference between luminance and chrominance channels as the result of denoising procedure. In this approach they introduce the concept of directional "demosaicing noise" for the interpolation errors and filter it.

In case of treating the original noisy observed data the denoising done first was proven to be more efficient. Some post-CFAI noise reduction (NR) and pre-CFAI NR techniques are compared in¹³. The authors show the possibility to reduce more noise with the pre-CFAI NR methods than with the post-CFAI NR methods and propose a new solution for improving the detail preserving properties of the pre-CFAI NR filters like a simple detail detector. The computational costs can be lower with the pre-CFAI NR methods than with the post-CFAI NR methods. For instance, a single-channel image is processed before interpolation, while three color channels should be denoised on a post-CFAI stage. The model of noise plays an important role in image denoising, which is known before CFAI but not after CFAI. Authors say that also the level of sharpness provided by the post-CFAI NR methods could be maintained or even improved with the pre-CFAI NR methods^{13,14}.

Noting that image interpolation and image denoising are both estimation problems, the paper² proposes a unified approach to performing demosaicing and image denoising jointly, where the noise is modeled as multiplicative Gaussian. The multi-colored demosaicing/denoising problem was simplified to a single-color denoising problem. A Total Least Squares algorithm was designed to solve this problem. The authors verified that performing demosaicing and denoising jointly is more effective than treating them independently². Ramanath and Snyder¹⁵ proposed a bilateral filtering based scheme to denoise, sharpen and demosaic the image simultaneously. We follow this principle and target to design a novel joint demosaicing and denoising approach.

This paper is inspired by the work of Zhang and Wu¹¹ on directional linear minimum mean square-error estimation (DLMMSE) based CFAI targeted noiseless Bayer-patterned data. The authors proposed to find estimates of difference between luminance and chrominance channels as the result of directional filtering of interpolation errors.

Most of denoising techniques are designed for stationary Gaussian distributed noise. However, often this model does not correspond to reality and the quality of restoration is negatively affected by such mismatch. More realistic models describe the noise in CCD and CMOS sensors as signal-dependant^{2,16,17,18}. We propose a denoising technique specially designed for filtering not only Gaussian but also signal-dependant noise. The approach is based on the adaptive LPA-ICI technique¹⁶. Instead of denoising the R , G , and B , channels independently, our technique effectively exploits the high correlation between the three color channels.

Firstly, we compute initial directional interpolated estimates of noisy color intensities. Afterward, these estimates are decorrelated and denoised by the special directional anisotropic filters. This approach is found to be efficient in order to attenuate both noise and interpolation errors. The exploited denoising technique is based

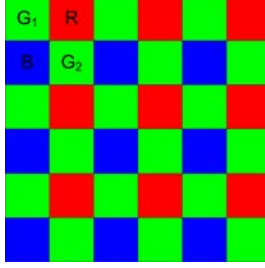


Figure 1. Bayer color filter array.

on the LPA. The adaptivity to data is provided by the multiple hypothesis testing called the ICI rule which is applied for adaptive selection of varying scales (window sizes) of LPA^{19,20,21}.

The proposed technique results in better utilization of data, in better performance and quality of image restoration, and lower complexity of implementation. These issues are of crucial importance especially for small mobile devices, where the impact of noise is particularly severe because of the constrained power and hardware.

In this work, noise is treated as an important intrinsic degradation of the data. Nevertheless, a similar approach can be successfully exploited also for CFAI of noise free data. We refer the reader to our work²², where we present an adaptation of our method which takes significant advantage from assuming that the data is noise free.

2. IMAGE FORMATION MODEL

We follow the general Bayer mask image formation model:

$$z_{bayer}(i, j) = \Psi\{y_{RGB}(i, j)\} + \sigma_{bayer}(i, j)n(i, j). \quad (1)$$

where $\Psi\{\cdot\}$ is a Bayer sampling operator¹:

$$\Psi\{y_{RGB}(i, j)\} = \begin{cases} G(i, j), & \text{at } (i, j) \in X_{G_1}, \\ G(i, j), & \text{at } (i, j) \in X_{G_2}, \\ R(i, j), & \text{at } (i, j) \in X_R, \\ B(i, j), & \text{at } (i, j) \in X_B, \end{cases} \quad (2)$$

and z_{bayer} is the output signal of the sensor, $y_{RGB}(i, j) = (R(i, j), G(i, j), B(i, j))$ is a true color RGB observation scene, $X = \{(i, j) : i = 1, \dots, 2N, j = 1, \dots, 2M\}$ are the spatial coordinates and R , G , and B correspond to the color channels. Further, for the two green channels we will use notations $G_1(i, j)$, such that $(i, j) \in X_{G_1} = \{(i, j) : i = 1, 3, \dots, 2N - 1, j = 1, 3, \dots, 2M - 1\}$, and $G_2(i, j)$, such that $(i, j) \in X_{G_2} = \{(i, j) : i = 2, 4, \dots, 2N, j = 2, 4, \dots, 2M\}$. Spatial coordinates for the red $R(i, j)$ and blue $B(i, j)$ color channels are denoted $X_R = \{(i, j) : i = 1, 3, \dots, 2N - 1, j = 2, 4, \dots, 2M\}$ and $X_B = \{(i, j) : i = 2, 4, \dots, 2N, j = 1, 3, \dots, 2M - 1\}$, respectively. The term $n(i, j)$ is an independent zero-mean noise with variance equal to one at every point (i, j) . Thus, $\sigma_{bayer}(i, j)$ is the standard deviation of $z_{bayer}(i, j)$. It is not necessarily constant with respect to the spatial variable (i, j) .

In this paper, we consider the problem of reconstruction of the true color image y_{RGB} from the noisy sampled data z_{bayer} .

3. INITIALIZATION

Firstly we calculate the directional (horizontal and vertical) estimates of green channel at every point $(i, j) \in X$ following the rules of Hamilton-Adams algorithm⁶. Interpolation of G at R positions is done as follows:

$$\tilde{G}_h(i, j) = \frac{1}{2} (G(i+1, j) + G(i-1, j)) + \frac{1}{4} (-R(i-2, j) + 2R(i, j) - R(i+2, j)), \quad (3)$$

$$\tilde{G}_v(i, j) = \frac{1}{2} (G(i, j+1) + G(i, j-1)) + \frac{1}{4} (-R(i, j-2) + 2R(i, j) - R(i, j+2)). \quad (4)$$

Here h and v stay for horizontal and vertical estimates. Similarly, the initial directional estimates for the red channel R at green positions G ($(i, j) \in X_{G_1}$ or $(i, j) \in X_{G_2}$) are interpolated as:

$$\tilde{R}_h(i, j) = \frac{1}{2} (R(i+1, j) + R(i-1, j)) + \frac{1}{4} (-G(i-2, j) + 2G(i, j) - G(i+2, j)), \quad (5)$$

$$\tilde{R}_v(i, j) = \frac{1}{2} (R(i, j+1) + R(i, j-1)) + \frac{1}{4} (-G(i, j-2) + 2G(i, j) - G(i, j+2)). \quad (6)$$

Using the obtained estimates (3),(5) we have at the every horizontal line of R values two sets of values of green and red:

$$\begin{array}{ccccccc} \dots & \tilde{G}_h & G & \tilde{G}_h & G & \tilde{G}_h & \dots \\ \dots & R & \tilde{R}_h & R & \tilde{R}_h & R & \dots \end{array}.$$

Similar calculations are produced for the vertical lines.

Assuming that the color channels are correlated, we decorrelate them using the following standard summation and differentiation linear operators working in the horizontal direction:

$$\begin{pmatrix} \tilde{\Phi}_{g,r}^h(i, j) \\ \tilde{\Delta}_{g,r}^h(i, j) \end{pmatrix} = \begin{pmatrix} 1 & 1 \\ 1 & -1 \end{pmatrix} \begin{pmatrix} G(i, j) \\ \tilde{R}_h(i, j) \end{pmatrix}, \quad (i, j) \in X_{G_1}, \quad (7)$$

and in the vertical direction

$$\begin{pmatrix} \tilde{\Phi}_{g,r}^v(i, j) \\ \tilde{\Delta}_{g,r}^v(i, j) \end{pmatrix} = \begin{pmatrix} 1 & 1 \\ 1 & -1 \end{pmatrix} \begin{pmatrix} \tilde{G}_h(i, j) \\ R(i, j) \end{pmatrix}, \quad (i, j) \in X_R. \quad (8)$$

For the vertical directions, the corresponding $\hat{\Phi}_{g,r}^v(i, j)$ and $\hat{\Delta}_{g,r}^v(i, j)$ are calculated as follows:

$$\begin{pmatrix} \hat{\Phi}_{g,r}^v(i, j) \\ \hat{\Delta}_{g,r}^v(i, j) \end{pmatrix} = \begin{pmatrix} 1 & 1 \\ 1 & -1 \end{pmatrix} \begin{pmatrix} G(i, j) \\ \tilde{R}_v(i, j) \end{pmatrix}, \quad (i, j) \in X_{G_2}, \quad (9)$$

and

$$\begin{pmatrix} \tilde{\Phi}_{g,r}^v(i, j) \\ \tilde{\Delta}_{g,r}^v(i, j) \end{pmatrix} = \begin{pmatrix} 1 & 1 \\ 1 & -1 \end{pmatrix} \begin{pmatrix} \tilde{G}_v(i, j) \\ R(i, j) \end{pmatrix}, \quad (i, j) \in X_R. \quad (10)$$

We assume for further filtering that the directional differences between the green and red signals $\tilde{\Delta}_{g,r}^h(i, j)$, $\tilde{\Delta}_{g,r}^v(i, j)$ can be presented as the sums of the true values of these differences and the errors including the random observation noise in (1) and what is called the "directional demosaicing noise"¹¹:

$$\tilde{\Delta}_{g,r}^h(i, j) = \Delta_{g,r}^h(i, j) + \varepsilon_{g,r}^{\Delta,h}(i, j), \quad (i, j) \in X_R \cup X_{G_1}, \quad (11)$$

$$\tilde{\Delta}_{g,r}^v(i, j) = \Delta_{g,r}^v(i, j) + \varepsilon_{g,r}^{\Delta,v}(i, j), \quad (i, j) \in X_R \cup X_{G_2}, \quad (12)$$

where $\varepsilon_{g,r}^{\Delta,h}(i, j)$ and $\varepsilon_{g,r}^{\Delta,v}(i, j)$ are the errors and $\Delta_{g,r}^h(i, j)$ and $\Delta_{g,r}^v(i, j)$ are the true values of the corresponding differences.

The same modeling with the additive errors is assumed for sums $\tilde{\Phi}_{g,r}^h(i, j)$ and $\tilde{\Phi}_{g,r}^v(i, j)$:

$$\tilde{\Phi}_{g,r}^h(i, j) = \Phi_{g,r}^h(i, j) + \varepsilon_{g,r}^{\Phi,h}(i, j), \quad (i, j) \in X_R \cup X_{G_1}, \quad (13)$$

$$\tilde{\Phi}_{g,r}^v(i, j) = \Phi_{g,r}^v(i, j) + \varepsilon_{g,r}^{\Phi,v}(i, j), \quad (i, j) \in X_R \cup X_{G_2}, \quad (14)$$

where $\Phi_{g,r}^h(i, j)$ and $\Phi_{g,r}^v(i, j)$ are the true values of the summes and $\varepsilon_{g,r}^{\Phi,h}(i, j)$, $\varepsilon_{g,r}^{\Phi,v}(i, j)$ are the errors.

It is seen that (7)-(10) can be computed as a convolution of $z_{bayer}(i, j)$ with the linear FIR filters with the masks $f_\Phi = (-1, 2, 6, 2, -1)/4$ and $f_\Delta = (-1, 2, -2, 2, -1)/4$. For calculations of the variance of the sums $\tilde{\Phi}_{g,r}^h$, $\tilde{\Phi}_{g,r}^v$, and differences $\tilde{\Delta}_{g,r}^h$, $\tilde{\Delta}_{g,r}^v$ in (7)-(10) we assume that the random observation noise is dominant in

the errors in (11)-(14). Then the observation noise from (1) gives the following standard deviations for the sums $\tilde{\Phi}_{g,r}^h, \tilde{\Phi}_{g,r}^v$ (13),(14):

$$\sigma_{\tilde{\Phi}_{g,r}^h}(i,j) = \sqrt{(\sigma_{bayer}^2 \circledast f_\Phi^2)(i,j)}, \quad (i,j) \in X_R \cup X_{G_1}, \quad (15)$$

$$\sigma_{\tilde{\Phi}_{g,r}^v(i,j)} = \sqrt{(\sigma_{bayer}^2 \circledast (f_\Phi^T)^2)(i,j)}, \quad (i,j) \in X_R \cup X_{G_2}, \quad (16)$$

where "⊗" denotes the discrete convolution operator, the symbol "T" denotes the transpose operation, and $\sigma_{bayer}(i,j)$ is a noise standard deviation in (1). The standard deviations for the differences $\tilde{\Delta}_{g,r}^h, \tilde{\Delta}_{g,r}^v$ corresponding to the observation noise are computed as

$$\sigma_{\tilde{\Delta}_{g,r}^h}(i,j) = \sqrt{(\sigma_{bayer}^2 \circledast f_\Delta^2)(i,j)}, \quad (i,j) \in X_R \cup X_{G_1}, \quad (17)$$

$$\sigma_{\tilde{\Delta}_{g,r}^v(i,j)} = \sqrt{(\sigma_{bayer}^2 \circledast (f_\Delta^T)^2)(i,j)}, \quad (i,j) \in X_R \cup X_{G_2}. \quad (18)$$

The blue channel B is treated in the same way in order to calculate the directional sums and differences $\tilde{\Delta}_{g,b}^h, \tilde{\Delta}_{g,b}^v, \tilde{\Phi}_{g,b}^h, \tilde{\Phi}_{g,b}^v$ for $(G - B)$ and $(G + B)$.

4. SPATIALLY ADAPTIVE DENOISING OF DIRECTIONAL ESTIMATES

The spatially adaptive LPA-ICI filtering^{19,20,21} is exploited to denoise $\tilde{\Delta}_{g,r}^h, \tilde{\Delta}_{g,r}^v, \tilde{\Phi}_{g,r}^h, \tilde{\Phi}_{g,r}^v$ for R color channel, and $\tilde{\Delta}_{g,b}^h, \tilde{\Delta}_{g,b}^v, \tilde{\Phi}_{g,b}^h, \tilde{\Phi}_{g,b}^v$ for B color channel. In order to introduce this filtering in the form applicable for any input data assume for a moment that this input noisy data have the form:

$$z(i,j) = y(i,j) + \sigma(i,j)n(i,j), \quad (19)$$

where $(i,j) \in X$, $z(i,j)$ is a noisy observation, $y(i,j)$ is a true signal, $n(i,j)$ is an independent zero-mean noise with variance equal to one at every point (i,j) , and $\sigma(i,j)$ is a standard deviation of $z(i,j)$ at each point.

The LPA is a general tool for linear filter design, in particular for design of the directional filters of the given polynomial orders on the arguments i and j . Let $g_{s,\theta}$ be the impulse response of the 2D directional linear filter designed by the LPA²¹, where θ is a direction of smoothing and s is a scale parameter (window size of the filter)*. A set of the image estimates of different scales s and different directions θ are calculated by the convolution

$$\hat{y}_{s,\theta}(i,j) = (z \circledast g_{s,\theta})(i,j), \quad (20)$$

for $s \in S = \{s_1, s_2, \dots, s_J\}$, where $s_1 < s_2 < \dots < s_J$, and $\theta \in \Theta$.

The ICI rule is the algorithm for a proper selection of the scale (close to the optimal value) for every pixel (i,j) ²¹. In the ICI rule a sequence of confidence intervals is used

$$D_s = [\hat{y}_{s,\theta}(i,j) - \Gamma\sigma_{\hat{y}_{s,\theta}}, \hat{y}_{s,\theta}(i,j) + \Gamma\sigma_{\hat{y}_{s,\theta}}], \quad s \in S, \quad (21)$$

where $\Gamma > 0$ is a threshold parameter for the ICI, the estimates and $\sigma_{\hat{y}_{s,\theta}}$ is the standard deviation of the estimate $\hat{y}_{s,\theta}$ calculated as

$$\sigma_{\hat{y}_{s,\theta}}(i,j) = \sqrt{(\sigma^2 \circledast g_{s,\theta}^2)(i,j)}, \quad (22)$$

where the weights are defined by $g_{s,\theta}$ used in (20).

*The MATLAB code that implements the LPA-ICI technique is available following the link: <http://www.cs.tut.fi/~lasip/>.

The rotated directional nonsymmetric kernel $g_{s,\theta}$ is used with the angle θ which defines the directionality of the filter, and scale s is a length of the kernel support (or a scale parameter of the kernel) in this direction.

The ICI rule defines the adaptive scale as the largest s^+ of those scales in S which estimate does not differ significantly from the estimates corresponding to the smaller window sizes. This optimization of s for each of the directional estimates yields the adaptive scales $s^+(\theta)$ for each direction θ . The union of the supports of $g_{s^+(\theta),\theta}$ is considered as an approximation of the best local vicinity of (i, j) in which the estimation model fits the data. The final estimate is calculated as a linear combination of the obtained adaptive directional estimates $\hat{y}_{s^+, \theta}(i, j)$.

The final LPA-ICI estimate $\hat{y}(i, j)$ combined from the directional ones is computed as the weighted mean

$$\hat{y}(i, j) = \sum_{\theta \in \Theta} \hat{y}_{s^+, \theta}(i, j) w_\theta, \quad w_\theta = \frac{\sigma_{\hat{y}_{s^+, \theta}}^{-2}}{\sum_{\theta \in \Theta} \sigma_{\hat{y}_{s^+, \theta}}^{-2}}, \quad (23)$$

with the variance $\sigma_{\hat{y}_{s^+, \theta}}^2$ of $\hat{y}(i, j)$ computed for simplicity as

$$\sigma_{\hat{y}_{s^+, \theta}}^2 = \left(\sum_{\theta \in \Theta} \sigma_{\hat{y}_{s^+, \theta}}^{-2} \right)^{-1}. \quad (24)$$

It is convenient to treat this complex LPA-ICI multidirectional algorithm as an adaptive filter two inputs z , and σ , and a single output \hat{y} . The input-output equation can be written as $\hat{y} = \mathcal{L}\mathcal{I}\{z, \sigma\}$ by denoting the calculations imbedded in this algorithm as an $\mathcal{L}\mathcal{I}$ operator.

Applying this $\mathcal{L}\mathcal{I}$ operator to calculated sums and differences we obtain the following denoised estimates of these difference: $\hat{\Delta}_{g,r}^h, \hat{\Delta}_{g,r}^v, \hat{\Phi}_{g,r}^h, \hat{\Phi}_{g,r}^v$ for R color channel, and $\hat{\Delta}_{g,b}^h, \hat{\Delta}_{g,b}^v, \hat{\Phi}_{g,b}^h, \hat{\Phi}_{g,b}^v$ for B color channel. When all the LPA-ICI estimates $\hat{\Delta}_{g,r}^h = \mathcal{L}\mathcal{I}\{\tilde{\Delta}_{g,r}^h, \sigma_{\tilde{\Delta}_{g,r}^h}\}, \hat{\Phi}_{g,r}^h = \mathcal{L}\mathcal{I}\{\tilde{\Phi}_{g,r}^h, \sigma_{\tilde{\Phi}_{g,r}^h}\}$, where the standard deviations $\sigma_{\tilde{\Delta}_{g,r}^h}, \sigma_{\tilde{\Phi}_{g,r}^h}$ are calculated according to (15)-(18), etc., are obtained they can be used to calculate R , G , and B color components at every position (i, j) .

5. INTERPOLATION OF G COMPONENT AT R/B POSITIONS AND DENOISING OF R/B AT R/B POSITIONS

Aggregation of the horizontal and vertical LPA-ICI estimates of the sums and differences in the final estimates of the sums and difference is produced according to the formula

$$\hat{\Delta}_{g,r} = \frac{\sigma_{\hat{\Delta}_h}^{-2}}{\sigma_{\hat{\Delta}_h}^{-2} + \sigma_{\hat{\Delta}_v}^{-2}} \hat{\Delta}_{g,r}^h + \frac{\sigma_{\hat{\Delta}_v}^{-2}}{\sigma_{\hat{\Delta}_h}^{-2} + \sigma_{\hat{\Delta}_v}^{-2}} \hat{\Delta}_{g,r}^v, \quad (25)$$

where $\hat{\Delta}_{g,r}^h = \mathcal{L}\mathcal{I}\{\tilde{\Delta}_{g,r}^h, \sigma_{\tilde{\Delta}_{g,r}^h}\}, \hat{\Delta}_{g,r}^v = \mathcal{L}\mathcal{I}\{\tilde{\Delta}_{g,r}^v, \sigma_{\tilde{\Delta}_{g,r}^v}\}$, and $\sigma_{\hat{\Delta}_h}, \sigma_{\hat{\Delta}_v}$ are the corresponding standard deviations of $\hat{\Delta}_{g,r}^h, \hat{\Delta}_{g,r}^v$ calculated as in (24). Aggregation of the horizontal and vertical LPA-ICI estimates $\hat{\Phi}_{g,r}^h, \hat{\Phi}_{g,r}^v$ in the final estimate $\hat{\Phi}_{g,r}$ is performed in analogous way to (25).

When the estimates of the sums and the differences are calculated we invert the formulas (7)-(10) in order to calculate the signals from these sums and differences. Both interpolation of G at R positions and denoising of R are performed as follows:

$$\begin{pmatrix} \hat{G}(i, j) \\ \hat{R}(i, j) \end{pmatrix} = \frac{1}{2} \begin{pmatrix} 1 & 1 \\ 1 & -1 \end{pmatrix} \begin{pmatrix} \hat{\Phi}_{g,r}(i, j) \\ \hat{\Delta}_{g,r}(i, j) \end{pmatrix}, \quad (i, j) \in X_R, \quad (26)$$

where \hat{G} and \hat{R} are the obtained color estimates.

Similar adaptive LPA-ICI filtering is applied for the B channel with the following reconstruction of the interpolated and denoised signals according to the formula analogous to (26).

6. DENOISING OF G COLOR

At every point $(i, j) \in X_{G_1}$ or $(i, j) \in X_{G_2}$ we have only vertical or horizontal sums and differences. For instance, it is easy to see from (11)-(14) that at G_1 positions $(i, j) \in X_{G_1}$ we have only horizontal $(G_1 + \tilde{R}_h), (G_1 - \tilde{R}_h)$, and vertical $(G_1 + \hat{B}_v), (G_1 - \tilde{B}_v)$:

$$\begin{cases} \tilde{\Phi}_{g,r}^h = G_1 + \tilde{R}_h, \quad \tilde{\Delta}_{g,r}^h = G_1 - \tilde{R}_h, \\ \tilde{\Phi}_{g,b}^v = G_1 + \hat{B}_v, \quad \tilde{\Delta}_{g,b}^v = G_1 - \tilde{B}_v, \end{cases}$$

and similarly

$$\begin{cases} \tilde{\Phi}_{g,r}^v = G_2 + \tilde{R}_v, \quad \tilde{\Delta}_{g,r}^v = G_2 - \tilde{R}_v, \\ \tilde{\Phi}_{g,b}^h = G_2 + \tilde{B}_h, \quad \tilde{\Delta}_{g,b}^h = G_2 - \tilde{B}_h, \end{cases}$$

at G_2 positions. The aggregation of the estimates of $\tilde{\Phi}_{g,r}^h, \tilde{\Delta}_{g,r}^h, \tilde{\Phi}_{g,b}^v, \tilde{\Delta}_{g,b}^v, \tilde{\Phi}_{g,r}^v, \tilde{\Delta}_{g,r}^v, \tilde{\Phi}_{g,b}^h, \tilde{\Delta}_{g,b}^h$, obtained by the LPA-ICI gives the final denoised estimate of green color component as the weighted mean:

$$\begin{cases} \hat{G} = \frac{1}{2}(\hat{\Phi}_{g,r}^h + \hat{\Delta}_{g,r}^h)w_{g,r}^h + \frac{1}{2}(\hat{\Phi}_{g,b}^v + \hat{\Delta}_{g,b}^v)w_{g,b}^v, & (i, j) \in X_{G_1}, \\ \hat{G} = \frac{1}{2}(\hat{\Phi}_{g,r}^v + \hat{\Delta}_{g,r}^v)w_{g,r}^v + \frac{1}{2}(\hat{\Phi}_{g,b}^h + \hat{\Delta}_{g,b}^h)w_{g,b}^h, & (i, j) \in X_{G_2}. \end{cases} \quad (27)$$

This estimate utilizes both R and B spectral components. Here, $\hat{\Phi}_{g,r}^h = \mathcal{LI}\left\{\tilde{\Phi}_{g,r}^h, \sigma_{\tilde{\Phi}_{g,r}^h}\right\}$, $\hat{\Delta}_{g,r}^h = \mathcal{LI}\left\{\tilde{\Delta}_{g,r}^h, \sigma_{\tilde{\Delta}_{g,r}^h}\right\}$, and analogously for $\hat{\Phi}_{g,r}^v, \hat{\Delta}_{g,r}^v, \hat{\Phi}_{g,b}^v, \hat{\Delta}_{g,b}^v, \hat{\Phi}_{g,b}^h, \hat{\Delta}_{g,b}^h$. The weights $w_{g,r}^h, w_{g,b}^v, w_{g,r}^v, w_{g,b}^h$ are computed using variances

$$\begin{cases} w_{g,r}^h = \sigma_{\hat{\Phi}_{g,r}^h}^{-2} / \left(\sigma_{\hat{\Phi}_{g,r}^h}^{-2} + \sigma_{\hat{\Phi}_{g,b}^v}^{-2} \right), \quad w_{g,b}^v = \sigma_{\hat{\Phi}_{g,b}^v}^{-2} / \left(\sigma_{\hat{\Phi}_{g,r}^h}^{-2} + \hat{\sigma}_{\hat{\Phi}_{g,b}^v}^{-2} \right), & (i, j) \in X_{G_1}, \\ w_{g,r}^v = \sigma_{\hat{\Phi}_{g,r}^v}^{-2} / \left(\sigma_{\hat{\Phi}_{g,r}^v}^{-2} + \sigma_{\hat{\Phi}_{g,b}^h}^{-2} \right), \quad w_{g,b}^h = \sigma_{\hat{\Phi}_{g,b}^h}^{-2} / \left(\sigma_{\hat{\Phi}_{g,r}^v}^{-2} + \sigma_{\hat{\Phi}_{g,b}^h}^{-2} \right), & (i, j) \in X_{G_2}, \end{cases}$$

calculated according to (24).

7. INTERPOLATION OF R/B AT B/R POSITIONS

For the interpolation of R/B colors at B/R positions we propose to use a special shift invariant interpolation filter giving the estimates by the standard convolution. The filters were designed for the subsampled grid which corresponds to R/B channel. A variety of polynomial orders and support sizes have been tested. As a result, the second order polynomial interpolation filter g_{rb} has been chosen:

$$g_{rb} = \begin{bmatrix} 0 & 0 & -0.0313 & 0 & -0.0313 & 0 & 0 \\ 0 & 0 & 0 & 0 & 0 & 0 & 0 \\ -0.0313 & 0 & 0.3125 & 0 & 0.3125 & 0 & -0.0313 \\ 0 & 0 & 0 & 0 & 0 & 0 & 0 \\ -0.0313 & 0 & 0.3125 & 0 & 0.3125 & 0 & -0.0313 \\ 0 & 0 & 0 & 0 & 0 & 0 & 0 \\ 0 & 0 & -0.0313 & 0 & -0.0313 & 0 & 0 \end{bmatrix} \quad (28)$$

as the one which provided the best performance. Finally, the interpolation of R/B color at B/R positions is performed exploiting obtained G values as follows:

$$\hat{R}(i, j) = \hat{G}(i, j) - (\hat{\Delta}_{g,r} \circledast g_{rb})(i, j), \quad (i, j) \in X_B, \quad (29)$$

$$\hat{B}(i, j) = \hat{G}(i, j) - (\hat{\Delta}_{g,b} \circledast g_{rb})(i, j), \quad (i, j) \in X_R, \quad (30)$$

where $\hat{G}(i, j)$ is obtained as in (26) and $\hat{\Delta}_{g,r}, \hat{\Delta}_{g,b}$ as in (25).

		07	08	13	19	23	Mean PSNR
HA ⁶ with prefiltering ²⁰	R	30.29	26.50	24.56	29.11	31.93	28.48
	G	31.06	27.30	24.79	29.94	32.66	29.15
	B	29.60	26.17	24.69	29.34	30.77	28.11
AP ⁹ with prefiltering ²⁰	R	30.51	27.24	25.25	29.35	31.96	28.86
	G	31.06	27.97	25.37	30.11	32.60	29.42
	B	30.53	27.39	25.65	30.09	31.93	29.12
DLMMSE ¹¹ with prefiltering ²⁰	R	30.89	27.51	25.40	29.66	32.34	29.16
	G	31.48	28.19	25.39	30.36	33.08	29.70
	B	31.00	27.65	25.75	30.36	32.39	29.43
Proposed LPA-ICI based interpolation	R	32.10	27.81	27.64	30.11	33.20	30.18
	G	32.47	28.70	27.73	30.86	34.15	30.79
	B	32.05	27.91	27.53	30.76	33.36	30.32

Table 1. PSNR values for CFA interpolation of images corrupted by Gaussian noise.

8. INTERPOLATION OF R/B AT G POSITIONS

Analogously to described in Section 7 approach is used for interpolation of R/B colors at G positions $((i,j) \in X_{G_1} \cup X_{G_2})$. We use the simplest symmetrical interpolation kernel g :

$$g = \begin{bmatrix} 0 & 0.25 & 0 \\ 0.25 & 0 & 0.25 \\ 0 & 0.25 & 0 \end{bmatrix},$$

because the higher order interpolation kernels did not provide a significant improvement in restoration. Then, the interpolated estimate is computed as follows:

$$\begin{aligned} \hat{R}(i,j) &= \hat{G}(i,j) - ((\Delta_{g,r} \circledast g_{rb}) \circledast g)(i,j), \\ \hat{B}(i,j) &= \hat{G}(i,j) - ((\Delta_{g,b} \circledast g_{rb}) \circledast g)(i,j). \end{aligned}$$

where \hat{G} is a denoised estimate (26).

9. SIMULATION RESULTS

In our simulations we use the standard test images with the intensities $y(i,j)$ belonging to the range [0,1]. In this paper we consider the following two noise models:

- a) Additive stationary white Gaussian noise with the invariant standard deviation $\sigma(i,j)$ constant for all $(i,j) \in X$ and for all color intensities G_1 , G_2 , R , and B ;
- b) Signal-dependent Poissonian distributed noise with $\chi z_{bayer}(i,j) \sim \mathcal{P}(\chi \Psi\{y_{RGB}(i,j)\})$. This noise can be written explicitly in the additive form (1) where the standard deviation depends on the image intensity as $\sigma(i,j) = \text{std}\{z_{bayer}(i,j)\} = \sqrt{\chi \Psi\{y_{RGB}(i,j)\}}$. It is shown in^{16,17,18} that such a model can be used for generic CMOS digital imaging sensors.

In particular, for the presented experiments we used $\sigma(i,j) = 0.05$ for the Gaussian model (a) and $\chi = 138.89$ for the Poissonian model (b).

The LPA-ICI filtering $\mathcal{L}\mathcal{I}\{\cdot\}$ is exploited for the eight directions $\theta \in \Theta = \{k \cdot 2\pi/8 : k = 0, \dots, 7\}$ with the scale (window size) values given by the set $S = \{1, 2, 4, 7, 10\}$. The threshold parameter Γ of the ICI rule is fixed as $\Gamma = 1$ for filtering the sums and as $\Gamma = 1.5$ for filtering the differences.

		07	08	13	19	23	Mean PSNR
HA ⁶ with prefiltering ³	R	30.07	25.72	25.00	28.17	31.59	28.11
	G	31.01	26.61	25.60	29.07	32.57	28.96
	B	29.87	25.42	24.93	28.61	30.79	27.92
AP ⁹ with prefiltering ³	R	30.42	26.49	26.07	28.53	31.85	28.67
	G	31.13	27.16	26.55	29.33	32.56	29.34
	B	30.77	26.56	26.26	29.30	31.85	28.94
DLMMSE ¹¹ with prefiltering ³	R	30.75	26.67	26.34	28.68	32.11	28.91
	G	31.53	27.45	26.66	29.52	33.02	29.63
	B	31.29	26.81	26.52	29.59	32.49	29.33
Proposed LPA-ICI based interpolation	R	31.76	27.17	27.18	29.39	32.59	29.62
	G	32.36	27.94	27.29	30.13	33.42	30.23
	B	32.08	27.28	27.10	30.15	32.85	29.89

Table 2. PSNR values for CFA interpolation of images corrupted by signal-dependent noise.

The results are shown in Tables 1,2 for five test images of the sizes 512×768 . The PSNR criterion is calculated excluding 15 border pixels in order to eliminate boundary effects. The mean PSNR values calculated over the five test images are given in the last column "Mean PSNR" of the table.

The PSNR values for the case of the Gaussian noise are shown in Table 1. The proposed algorithm is compared versus: Hamilton-Adams ("HA")⁶, Alternating Projections ("AP")⁹, and the DLMMSE algorithm ("DLMMSE")¹¹ with the LPA-ICI prefiltering of the noisy data²⁰. This prefiltering is applied to each color channel independently as the preprocessing stage. It is seen that in average (the last line of the table) the proposed integrated denoising and demosaicing technique provides PSNR at least 1 dB better than others algorithms. The LPA-ICI prefiltering for the Hamilton-Adams, DLMMSE and Alternating Projections algorithm have been chosen in order to make an objective comparison between the proposed algorithm designed for noisy data and the considered alternatives known as very good demosaicing algorithms designed for noiseless data.

The PSNR values for restoration of Bayer data corrupted by signal-dependant Poissonian type of noise are given in Table 2. For comparison we use the same alternative algorithms. For fair comparison we use the prefiltering of data for these algorithms. As the noise is signal dependent we use for this prefiltering a special recursive version of the LPA-ICI filtering developed specifically for observations with the signal dependent noise^{3,21}. In the result in Table 2 four iterations of this recursive prefiltering is used for the prefiltering. It is seen that from Table 2 that the proposed denoising-interpolation technique provides at least 0.6 dB better PSNR values that the alternative algorithms with the noise prefiltering. Note, that the proposed algorithm is non-recursive.

Visual comparison of the results is important for algorithm evaluation. Fig.2,3 illustrate some difficult parts of the restored Lighthouse test-image. Due to the denoising performed independently for each color channels the final image visually looks oversmoothed and suffers from color artefacts visible especially at edges (second and third columns), even for very advanced CFAI techniques. In combination with aliasing problem (noticeable at the fence and wall regions of the Lighthouse image) the color artefacts become visible significantly. In the case of Poissonian noise this problem arises even stronger. It is seen that the proposed technique (right column) provides significantly better performance also at the regions that contains small details and textures difficult for restoration.

The LPA-ICI denoising embedded into the interpolation procedure helps to avoid or reduce the mentioned above problems. As a result numerical ("LPA-ICI" row of Tables 1,2) and visual (Fig.2,3 right column) quality evaluation shows better performance. The high frequency regions difficult for denoising like the grass region are preserved significantly better and color artefacts are reduced. As a result the restored image looks more natural.

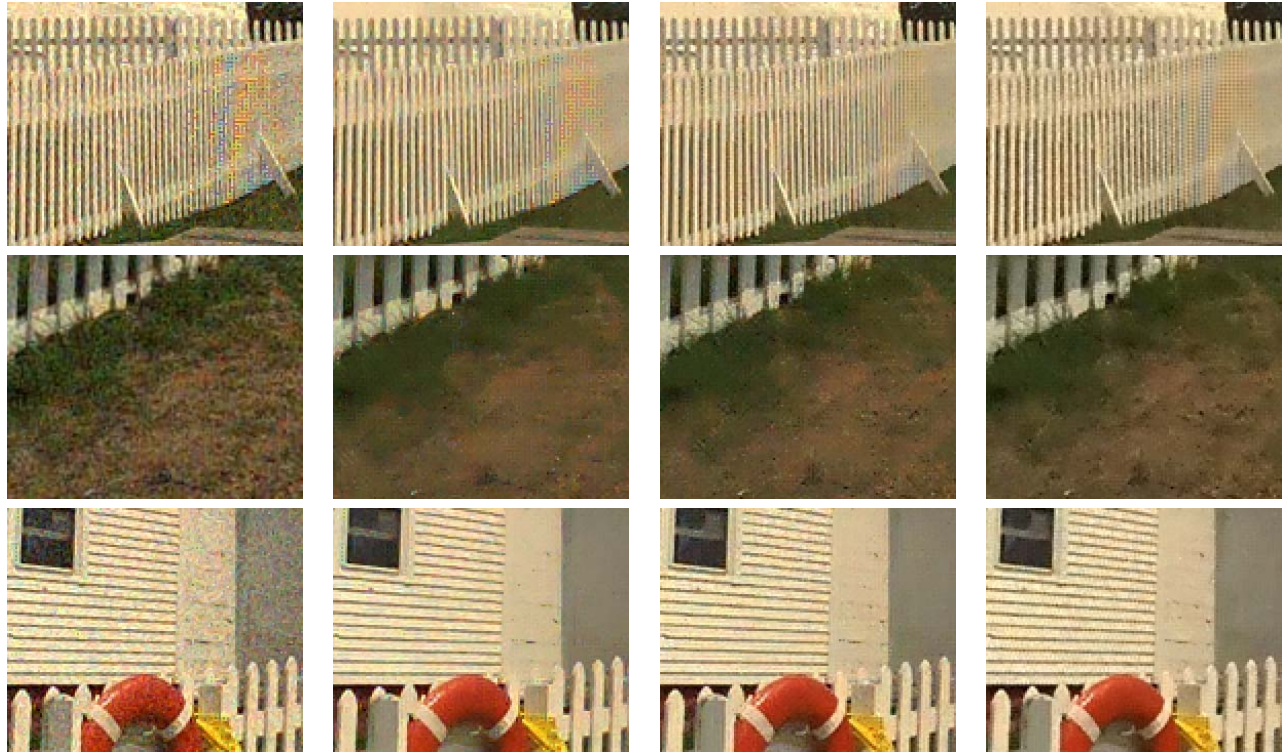


Figure 2. Restoration of the Lighthouse test image corrupted by Gaussian noise with $\sigma=0.05$. Columns are enumerated from left to right: interpolated noisy image by HA⁶ CFAI; restoration by HA⁶ CFAI with LPA-ICI²⁰ denoising at the prefiltering step, PSNR=(29.11, 29.94, 29.34); restoration by AP⁹ CFAI with LPA-ICI²⁰ denoising at the prefiltering step, PSNR=(29.35, 30.11, 30.09); restoration by DLMMSE¹¹ CFAI with LPA-ICI²⁰ denoising at the prefiltering step, PSNR=(29.66, 30.36, 30.36); proposed LPA-ICI based integrated interpolation and denoising, PSNR=(30.11, 30.86, 30.76).

10. ACKNOWLEDGMENTS

This work was supported by the Finnish Funding Agency for Technology and Innovation (Tekes). The authors thank Dr. Alessandro Foi for useful and practical discussions, and Dr. Lei Zhang for providing the implementation code of the technique¹¹.

REFERENCES

1. B.E. Bayer, "Color imaging array," U.S. Patent 3 971 065, July 1976.
2. K. Hirakawa, T.W. Parks, "Joint Demosaicing and Denoising", IEEE ICIP 2005, III, pp. 309-312, 2005.
3. Foi A., R. Bilcu, V. Katkovnik, and K. Egiazarian, "Anisotropic local approximations for pointwise adaptive signal-dependent noise removal", Proc. XIII European Signal Process. Conf., EUSIPCO 2005, Antalya, September 2005.
4. J.E. Adams Jr., "Design of color filter array interpolation algorithms for digital cameras, Part 2," in IEEE Proc. Int. Conf. Image Processing, vol. 1, Oct. 1998, pp. 488–492.
5. C.A. Laroche and M.A. Prescott, "Apparatus and method for adaptively interpolating a full color image utilizing chrominance gradients", U.S. Patent 5 373 322, Dec. 1994.
6. J.F. Hamilton Jr. and J.E. Adams, "Adaptive Color plane Interpolation in single color electronic camera", U.S. Patent 5 629 734, May 1997.
7. Malvar H.S., Li-wei He, and R. Cutler, "High-quality linear interpolation for demosaicing of Bayer-patterned color images", IEEE International Conference (ICASSP '04), Proceedings on Acoustics, Speech, and Signal Processing, Volume 3, Page(s):iii - 485-8, 17-21 May 2004.

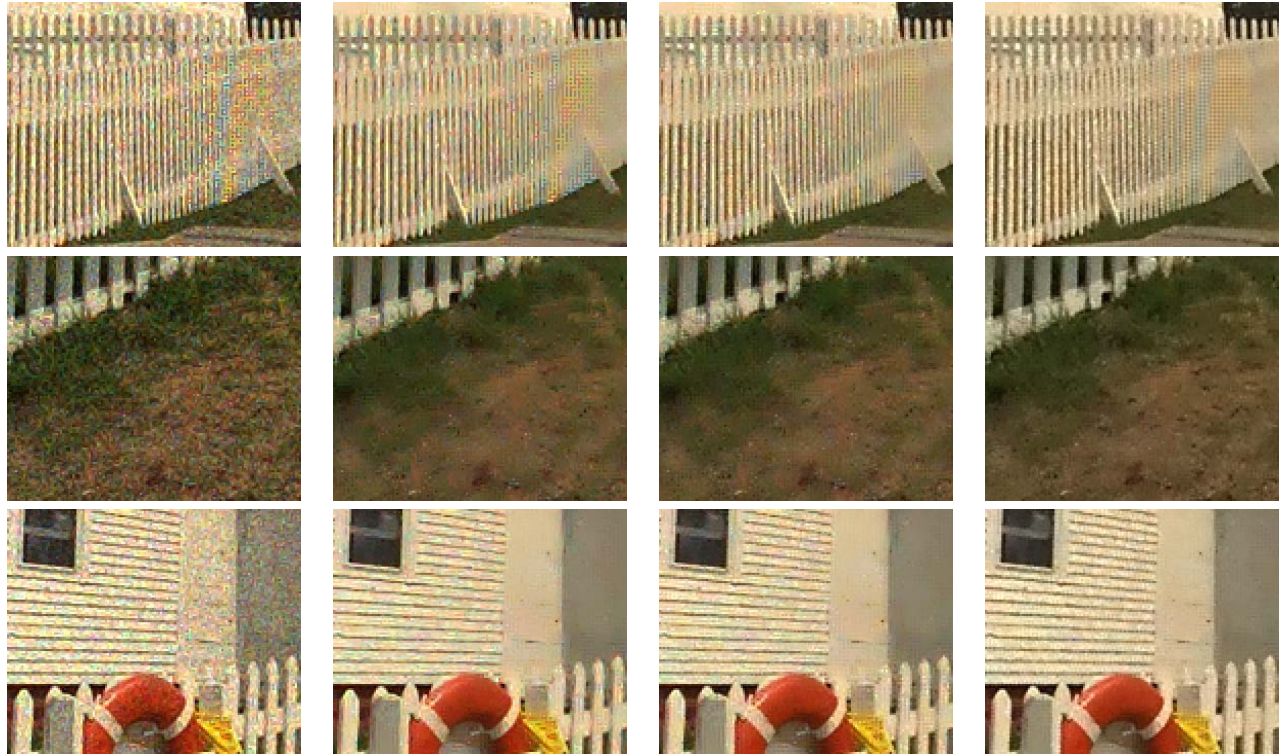


Figure 3. Restoration of the Lighthouse test image corrupted by signal-dependant noise. Columns are enumerated from left to right: interpolated noisy image by HA⁶ CFAI; restoration by HA⁶ CFAI with iterative LPA-ICI denoising³ at the prefiltering step, PSNR=(28.17, 29.07, 28.61); restoration by AP⁹ CFAI with iterative LPA-ICI denoising³ at the prefiltering step, PSNR=(28.53, 29.33, 29.30); restoration by DLMMSE¹¹ CFAI with iterative LPA-ICI denoising³ at the prefiltering step, PSNR=(28.68, 29.52, 29.59); proposed LPA-ICI based integrated interpolation with denoising, PSNR=(29.39, 30.13, 30.15).

8. Wu X., N. Zhang, "Primary-consistent soft-decision color demosaicking for digital cameras (patent pending)", *IEEE Transactions on Image Processing*, Volume 13, Issue 9, Page(s):1263 - 1274, Sept. 2004.
9. Gunturk B.K., Y. Altunbasak, R.M. Mersereau, "Color plane interpolation using alternating projections", *IEEE Transactions on Image Processing*, Volume 11, Issue 9, Page(s):997 - 1013, Sept. 2002.
10. Xin Li, "Demosaicing by successive approximation", *IEEE Transactions on Image Processing*, Volume 14, Issue 3, Page(s):370 - 379, March 2005.
11. L. Zhang, X. Wu, "Color Demosaicking Via Directional Linear Minimum Mean Square-Error Estimation", *IEEE Transactions on Image Processing*, Vol. 14, No. 12, pp. 2167-2178, December 2005.
12. Hirakawa K., T.W. Parks, "Adaptive homogeneity-directed demosaicing algorithm", *IEEE Transactions on Image Processing*, Volume 14, Issue 3, Page(s):360 - 369, March 2005.
13. O. Kalevo, H. Rantanen, "Noise Reduction Techniques for Bayer-Matrix Images", Sensors and Camera systems for scientific, industrial, and digital photography applications III, Proceedings of SPIE vol. 4669, 2002.
14. O. Kalevo, H. Rantanen, "Sharpening Methods for Images Captured through Bayer Matrix", Sensors, Cameras, and Applications for Digital Photography V, IS&T/SPIE's Electronic Imaging Science and Technology conference 2003, Santa Clara, 2003.
15. Ramanath R., Snyder W.E., "Adaptive Demosaicking", *J. Electron. Imag.*, Vol. 12, No. 4, pp. 633-642, 2003.
16. Foi A., V. Katkovnik, D. Paliy, K. Egiazarian, M. Trimeche, S. Alenius, R. Bilcu, M. Vehvilainen, "Apparatus, method, mobile station and computer program product for noise estimation, modeling and filtering of a digital image", U.S. Patent (Application No. 11/426,128, June 2006).

17. Foi, A., M. Trimeche, V. Katkovnik, and K. Egiazarian, "A Poissonian noise model for the raw-data of digital imaging sensors", (*submitted, in review*) *IEEE Sensors J.*, December 2006.
18. Foi, A., S. Alenius, V. Katkovnik, and K. Egiazarian, "Noise measurement for raw-data of digital imaging sensors by automatic segmentation of non-uniform targets", (*submitted, in review*) *IEEE Sensors J.*, December 2006.
19. V. Katkovnik, "A new method for varying adaptive bandwidth selection", *IEEE Trans. on Signal Proc.*, vol. 47, no. 9, pp. 2567-2571, 1999.
20. V. Katkovnik, K. Egiazarian, and J. Astola, "Adaptive window size image de-noising based on intersection of confidence intervals (ICI) rule", *J. of Math. Imaging and Vision*, vol. 16, no. 3, pp. 223-235, 2002.
21. V. Katkovnik, K. Egiazarian, and J. Astola, *Local Approximation Techniques in Signal and Image Processing*, SPIE Press, Monograph Vol. PM157, Hardcover, 576 pages, ISBN 0-8194-6092-3, September 2006.
22. Paliy D., R. Bilcu, V. Katkovnik, M. Vehvilainen, "Color Filter Array Interpolation Based on Spatial Adaptivity", Proc. SPIE Electronic Imaging 2007, Computational Imaging IV, 6497-7, San Jose, CA, January 2007.